Communications

Oxygen Electroreduction Catalyzed by Gold Nanoclusters: Strong Core Size Effects**

Wei Chen and Shaowei Chen*

In fuel cells, both the oxidation of small organic fuel molecules at the anode and the reduction of oxygen at the cathode necessitate effective electrocatalysts to achieve the current density needed for practical applications. Toward this end, platinum metal and platinum-based alloys have been examined extensively as active catalysts for both anode and cathode reactions. However, despite extensive research progress, wide-spread commercialization of fuel cells has been hindered by the sluggish reaction dynamics and by the high cost and limited supply of platinum. Therefore, in recent years, a number of studies have focused on non-platinum electrocatalysts.[1–5]

Compared to the platinum-group metals, bulk gold has attracted little attention in electrocatalysis, largely because of its poor catalytic performance. However, when the dimensions of the gold catalysts are diminished to the nanoscale, the materials properties exhibit a dramatic deviation from those of bulk Au.[6] Consequently, nanosized gold particles (diameters smaller than 10 nm) have been examined rather extensively as active catalysts for CO oxidation[7–9] and oxygen reduction.[10,11] The unusual catalytic activity of gold nanoparticles has been largely accounted for by the high fraction of surface atoms with low coordination numbers, which can be manipulated readily by altering the nanoparticle dimensions. Therefore, several studies have evaluated the effect of size on nanoparticle catalytic activity;[7,12,13] however, most of these earlier studies focused on Au nanoparticles that are larger than 2 nm in diameter. More recently, Herzing et al.[14] observed high catalytic activity in CO oxidation with gold clusters containing only about 10 gold atoms (ca. 0.5 nm in diameter). This work suggests that sub-nanometer-sized gold clusters might represent a unique class of catalysts that deserve further investigation.

Within this context, we prepared a series of Au nanoclusters with 11 to 140 gold atoms in the cores (0.8 to 1.7 nm in diameter) and carried out detailed electrochemical studies in alkaline media to evaluate the size effect on the electrocatalytic activity in oxygen reduction. It should be noted that

[*] Dr. W. Chen, Prof. S. Chen
Department of Chemistry and Biochemistry, University of California
Santa Cruz, CA 95064 (USA)
Fax: (+1) 831-459-2935
E-mail: schen@chemistry.ucsc.edu
Homepage: http://chemistry.ucsc.edu/~schen

Supporting information for this article is available on the WWW under http://dx.doi.org/10.1002/anie.200901185.

oxygen electroreduction is a reaction of tremendous interest for both basic research and technological applications in fuel cells, and previous work on the electrocatalysis of gold nanoparticles in oxygen reduction has mainly concentrated on much larger particles, the performance of which is generally poor.

Gold nanoclusters of varied sizes were first prepared according to well-established synthetic protocols (see the Supporting Information). Their detailed structures were examined by matrix-assisted laser desorption ionization (MALDI) mass spectrometry.[15–22] Note that it is difficult to study ultrasmall nanoparticles in the (sub)nanometer regime by TEM, and MALDI mass spectrometry has emerged as an indispensable tool in the accurate assessment of the particle core size. Figure 1 depicts a series of mass spectra of the
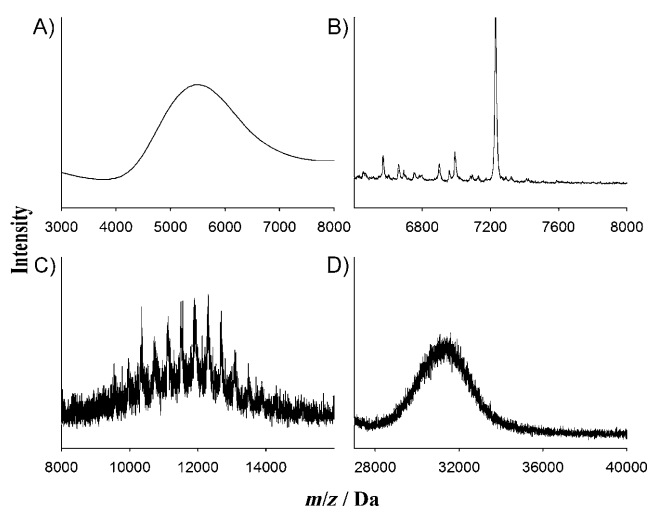
Figure 1. Positive MALDI-TOF mass spectra of A) Au_{11}, B) Au_{25}, C) Au_{55}, and D) Au_{140} nanoclusters with a *trans*-2-[3-(4-*tert*-butylphenyl)-2-methyl-2-propenylidene]malononitrile (DCTB) matrix.

various Au clusters. In Figure 1 A, the broad peak between 4 and 6 kDa is assigned to the $Au_{11}Cl_3(PPh_3)_8$ clusters (a series of sharp peaks at lower mass, below 2 kDa, were also observed, which were ascribed to Au_5, Au_9, and Au_{10} clusters that arose from desorption and ionization of the Au_{11} clusters by laser irradiation).[18] In Figure 1 B, the peak at around 7.2 kDa is in good agreement with the mass of $Au_{25}(SCH_2CH_2Ph)_{18}$ clusters, and those at lower mass correspond to the main fragments of the Au clusters as a result of laser irradiation. Figure 1 C shows the mass spectrum of $Au_{55}(PPh_3)_{12}Cl_6$ with a dominant maximum around 12 kDa. The peak spacing of about 400 Da might be attributed to the successive loss of two Au atoms between the fragments.[23] In

Figure 1 D, the dominant maximum increases to 31.5 kDa, in good agreement with the molecular weight of the $Au_{140}(S-(CH_2)_5CH_3)_{53}$ clusters. It should be noted that these mass spectrometric profiles are all consistent with previous studies in the quantitative determination of gold nanocluster core dimensions.[16,18–20,22] UV/Vis absorption spectroscopy measurements further confirmed the variation of the nanocluster core size (Figure S1 in the Supporting Information).

The electrocatalytic activity of these Au nanoclusters in oxygen reduction was then examined by cyclic voltammetry. The same amount by mass of gold nanoclusters was loaded onto a glassy carbon electrode (referred to as Au_x/GC), and all the currents were normalized to the effective Au surface areas, which were determined from the charge needed to form a gold surface oxide monolayer according to the oxygen adsorption measurement method.[24] Figure 2 shows the cyclic
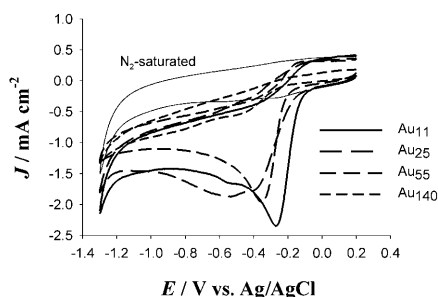
Figure 2. Cyclic voltammograms of the Au_x/GC electrodes ($x = 11$, 25, 55, and 140) in 0.1 M KOH saturated with oxygen and of the Au_{11}/GC electrode in N_2-saturated 0.1 M KOH solution (thin solid curve). Current density was calculated by normalizing the voltammetric currents to the effective Au active surface areas. Potential scan rate 0.1 Vs^{-1}.

voltammograms of the Au_x/GC electrode in an aqueous solution of 0.1 M KOH that was saturated with either N_2 or O_2 at a potential sweep rate of 0.1 Vs^{-1}. First, it can be seen that with the Au_{11}/GC electrode in the N_2-saturated solution (thin solid curve), the voltammetric currents were featureless within the potential range of -1.2 to $+0.2$ V (other electrodes showed similar results, not shown). In contrast, when the electrolyte solution was saturated with O_2, obvious reduction current started to appear with a rather well-defined cathodic peak, suggesting electrocatalytic activity of the gold nanoclusters in oxygen reduction.

It should be noted that the onset potential and peak current density, two important parameters in the quantitative assessments of electrocatalytic performance, vary sensitively with the core size of the Au clusters. For instance, for Au_{11} clusters, the onset potential of O_2 reduction was found to be approximately -0.08 V and the peak current density to be 2.4 mA cm^{-2}. However, for Au_{140} clusters, the onset potential shifted cathodically to -0.22 V, and the reduction peak current diminished to below 1.0 mA cm^{-2}. The catalytic activity of the Au_{25} and Au_{55} clusters appears to be in the intermediate range. That is, within the present experimental context, the electrocatalytic activity for O_2 reduction increases with decreasing core dimension of the gold nano-

clusters, with Au_{11} clusters being the most effective electrocatalysts.

Mechanistically, oxygen adsorption on the catalyst surface is the first step in electroreduction. Yet little O_2 can be adsorbed on bulk Au surfaces,[25] which is the main reason that bulk Au is not an active metal catalyst for oxygen reduction. However, for Au nanoparticles, the much lower coordination number of the surface atoms renders the nanoparticle surfaces more active than their smooth bulk counterparts. Therefore, their enhanced catalytic activity as described above may be ascribed, at least in part, to the large fraction of surface Au atoms with low coordination numbers. Furthermore, recent theoretical studies[26,27] have shown that with decreasing core size of Au nanoclusters, the d bands become narrowed and shift towards the Fermi level. This finding suggests that smaller Au clusters are energetically more favorable for O_2 adsorption, which may also account for the experimental results presented above. In fact, in a recent study of CO oxidation with gold nanocrystals using atomic-resolution scanning transmission electron microscopy,[14] it was found that the 0.5 nm Au clusters (ca. 10 gold atoms) were the actual contributors to the high activity for CO oxidation. Additionally, the fluxionality of nanosized metal particles may also contribute to the enhanced adsorption of oxygen.[28]

To further examine the effect of the core size of gold nanoclusters on their electrocatalytic activity in oxygen reduction, the reaction kinetics were evaluated and compared by rotating-disk voltammetry. Figure 3 A shows the rotating-disk voltammograms of oxygen reduction recorded at the Au_{11}/GC electrode in an oxygen-saturated 0.1 M KOH solution
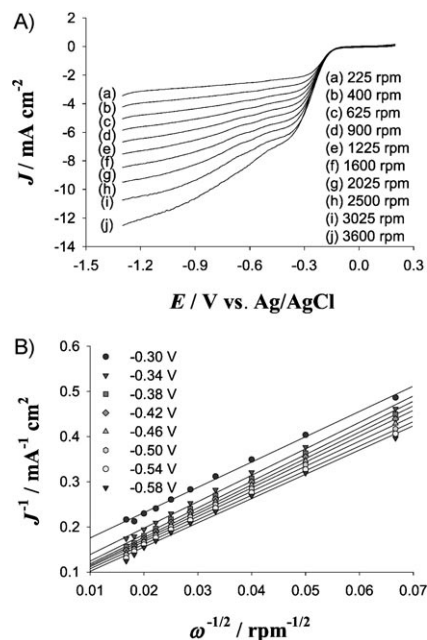
Figure 3. A) Rotating-disk voltammograms recorded for a GC electrode modified by Au_{11} clusters in aqueous 0.1 M KOH saturated with oxygen at different rotation rates. B) Koutecky–Levich plots (J^{-1} vs. $\omega^{-1/2}$) at different electrode potentials. DC ramp 20 mVs^{-1}. Symbols are experimental data obtained from (A), and lines are linear regressions.

at different rotation rates (from 225 to 3600 rpm). The current density plateaus are much better defined than those with larger Au nanoparticles;[13,29] overall, the voltammetric profiles are similar to those observed with Pt (or Pt-alloy)-based electrodes,[4] in which the current density increases with increasing rotation rates. The onset potential of oxygen reduction can be found to be approximately −0.1 V, which is close to that obtained from cyclic voltammetric measurements in Figure 2 (−0.08 V). Figure 3B depicts the corresponding Koutecky–Levich plots (J^{-1} vs. $\omega^{-1/2}$, see below) at various electrode potentials. It can be seen that the data exhibit good linearity, and the slopes remain approximately constant over the potential range of −0.58 to −0.30 V, thus suggesting consistent electron transfer for oxygen reduction at different electrode potentials. The linearity and parallelism of the plots is usually taken as an indication of first-order reaction kinetics with respect to dissolved O_2. The kinetic parameters can be analyzed with the Koutecky–Levich equations [Eqs. (1)–(3)]:

$$\frac{1}{J} = \frac{1}{J_L} + \frac{1}{J_K} = \frac{1}{B\omega^{1/2}} + \frac{1}{J_K} \tag{1}$$

$$B = 0.62\, n\, F\, C_O\, D_O^{2/3}\, \nu^{-1/6} \tag{2}$$

$$J_K = n\, F\, k\, C_O \tag{3}$$

where J is the measured current density, J_K and J_L are the kinetic and diffusion limiting current densities, respectively, ω is the electrode rotation rate, n is the overall number of electrons transferred in oxygen reduction, F is the Faraday constant, C_O is the bulk concentration of O_2 dissolved in the electrolyte, D_O is the diffusion coefficient of O_2, ν is the kinematic viscosity of the electrolyte, and k is the electron-transfer rate constant. According to Equations (1) and (2), the number of electrons transferred (n) and J_K can be obtained from the slope and intercept of the Koutecky–Levich plots, respectively. For instance, at the Au_{11}/GC electrode the number of electrons transferred was estimated to be 3.9 per O_2 molecule by using the values of $C_O = 1.2 \times 10^{-3}\ \mathrm{mol\,L^{-1}}$,[30] $D_O = 1.9 \times 10^{-5}\ \mathrm{cm^2\,s^{-1}}$,[30] and $\nu = 0.01\ \mathrm{cm^2\,s^{-1}}$[29] in 0.1 M KOH. The kinetic limiting current density (J_K) was calculated to be −17.9 mA cm^{-2} at −0.50 V (Table 1).

Figure 4 compares the rotating-disk voltammograms for oxygen reduction at other Au_x/GC electrodes (at the same
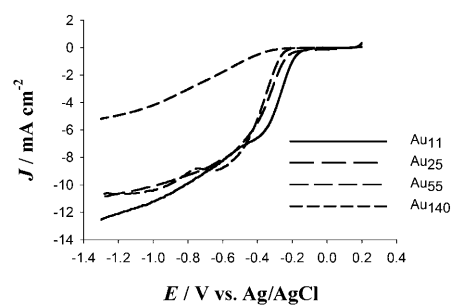
Figure 4. RDE voltammograms of varied Au_x/GC electrodes in 0.1 M KOH aqueous solution saturated by oxygen. Experimental conditions were the same as in Figure 3. Rotation rate 3600 rpm.

rotating rate of 3600 rpm). Strong core-size effects can be clearly seen, in good agreement with results from the voltammetric studies presented in Figure 2. First, the overall limiting current density (e.g., at −1.0 V) increases with decreasing particle core size: Au_{11}/GC (−11.2 mA cm^{-2}) > Au_{25}/GC (−10.1 mA cm^{-2}) ≈ Au_{55}/GC (−10.4 mA cm^{-2}) > Au_{140}/GC (−4.2 mA cm^{-2}). Notably, these values are all much higher than those with Au nanoparticles larger than 2 nm in diameter.[13,29] Second, with increasing Au cluster size, the onset potential of oxygen reduction shifts negatively: Au_{11}/GC (−0.10 V) > Au_{25}/GC (−0.16 V) > Au_{55}/GC (−0.20 V) > Au_{140}/GC (−0.25 V). Third, from linear regressions by the Koutecky–Levich equations (not shown), the electron-transfer kinetics of oxygen reduction also exhibit an apparent variation with gold cluster core size, as reflected by the apparent increase of kinetic limiting current density (J_K) with decreasing particle core dimensions, that is, at −0.5 V: Au_{11}/GC (−17.9 mA cm^{-2}) > Au_{25}/GC (−10.0 mA cm^{-2}) > Au_{55}/GC (−9.3 mA cm^{-2}) > Au_{140}/GC (−1.7 mA cm^{-2}). For comparison, Tang et al. reported kinetic current density of 3.5 and 1.5 mA cm^{-2} at −0.6 V (vs. Ag/AgCl) for oxygen reduction catalyzed by 3 and 7 nm Au clusters, respectively, in similar alkaline solutions.[13] Furthermore, the oxygen reduction reaction was found to proceed by the efficient four-electron reaction pathway with the smaller clusters (Au_{11}, Au_{25}, and Au_{55}), whereas incomplete reduction occurred with the largest one (Au_{140}), for which the two-electron reaction route was favored. These results are summarized in Table 1.

Overall, these Au nanoclusters exhibit much higher electrocatalytic activity for oxygen reduction, especially much larger reduction current density, than polycrystalline or single-crystalline Au catalysts and Au particles of larger dimensions.[13,29,31] Furthermore, the observed performance is highly comparable to that of some commercial Pt catalysts. For instance, in a recent study,[32] the onset potential of oxygen reduction was found at around −0.2 V (vs. Ag/AgCl) for commercial Pt catalysts loaded on carbon (Vulcan XC-72R), which is very close to the results presented above with gold nanoclusters (Table 1). These experimental observations suggest the potential application of atomic Au clusters as effective cathode catalysts in fuel-cell electrochemistry.

It should be noted that in the present study, the gold nanoclusters were all passivated by organic surfactants. Yet appreciable voltammetric currents were detected, suggesting ready access of oxygen to the particle surface and relatively

Table 1: Summary of the kinetic parameters for oxygen reduction at Au_x/GC electrodes.

Au_x	Au_{11}	Au_{25}	Au_{55}	Au_{140}
number of electrons transferred[a]	3.90	4.06	4.10	2.50
onset potential [V][b]	−0.10	−0.16	−0.20	−0.25
J_K at −0.50 V [mA cm^{-2}][c]	−17.9	−10.0	−9.3	−1.7

[a] The number of electrons transferred per O_2 molecule was calculated from Equations (1) and (2). [b] The onset potentials were determined from rotating-disk voltammograms (Figure 4). [c] The kinetic current density was derived from the Koutecky–Levich plots as exemplified in Figure 3B. On the basis of Equation (3), the rate constants (k) were estimated to be 3.96×10^{-2}, 2.13×10^{-2}, 1.96×10^{-2}, and 5.87×10^{-3} cm s^{-1} for $x = 11$, 25, 55, and 140, respectively.

low impedance to interfacial charge transfer. Furthermore, the fact that we were able to rinse the clusters off the electrode surface with organic solvents at the end of the experimental measurements indicated that the nanoparticle structures were stable throughout the procedure and thus that the nanocluster catalysts might be reusable. To further enhance the electrocatalytic activities, surface engineering will be needed to manipulate the nanocluster structure. This will be pursued in future work.

Experimental Section

UV/Vis spectroscopic studies were performed with an ATI Unicam UV4 spectrometer using a 1 cm quartz cuvette with a resolution of 2 nm. MALDI-TOF mass spectra were acquired using an Ettan MALDI-TOF Pro (Amersham Biosciences) spectrometer equipped with a standard UV nitrogen laser (337 nm). The accelerating voltage was held at 20 kV and positive ion mode was used. The Au cluster solutions in CH_2Cl_2 were mixed with the DCTB matrix (10 mg mL^{-1} in CH_2Cl_2) and then applied to the sample plate and air-dried.

A glassy carbon (GC) disk electrode (Bioanalytical Systems, 3.0 mm diameter) was first polished with alumina slurries (0.05 μm) and then cleaned by successive sonication in 0.1M HNO_3, H_2SO_4, and nanopure water for 10 min. Au clusters dissolved in CH_2Cl_2 (1.0 mg mL^{-1}, 10 μL) were then dropcast onto the clean GC electrode surface by a Hamilton microliter syringe (the resulting electrodes were denoted as Au$_x$/GC). The particle films were dried by a gentle nitrogen stream for 2 min. All electrochemical experiments were performed in a single-compartment glass cell using a standard three-electrode configuration. A Ag/AgCl (in 3M NaCl(aq), Bioanalytical Systems, MF-2052) and a Pt coil were used as the reference and counter electrodes, respectively. All electrode potentials in the present study were referred to the Ag/AgCl reference electrode. Cyclic voltammetry and rotating-disk voltammetry were carried out using a Bioanalytical Systems (BAS) Electrochemical Analyzer (Model 100B). Oxygen reduction was examined by first bubbling ultrahigh purity oxygen through the electrolyte solution for at least 15 min and then blanketing the solution with an oxygen atmosphere during the entire experimental procedure. All electrochemical experiments were carried out at room temperature.

[1] U. A. Paulus, A. Wokaun, G. G. Scherer, T. J. Schmidt, V. Stamenkovic, V. Radmilovic, N. M. Markovic, P. N. Ross, *J. Phys. Chem. B* **2002**, *106*, 4181.

[2] W. Chen, J. Kim, S. H. Sun, S. W. Chen, *Phys. Chem. Chem. Phys.* **2006**, *8*, 2779.

[3] W. Chen, J. M. Kim, S. H. Sun, S. W. Chen, *Langmuir* **2007**, *23*, 11303.

[4] W. Chen, J. M. Kim, S. H. Sun, S. W. Chen, *J. Phys. Chem. C* **2008**, *112*, 3891.

[5] Q. G. He, W. Chen, S. Mukerjee, S. W. Chen, F. Laufek, *J. Power Sources* **2009**, *187*, 298.

[6] M. Haruta, N. Yamada, T. Kobayashi, S. Iijima, *J. Catal.* **1989**, *115*, 301.

[7] M. Valden, X. Lai, D. W. Goodman, *Science* **1998**, *281*, 1647.

[8] B. E. Hayden, D. Pletcher, J. P. Suchsland, *Angew. Chem.* **2007**, *119*, 3600; *Angew. Chem. Int. Ed.* **2007**, *46*, 3530.

[9] F. Boccuzzi, G. Cerrato, F. Pinna, G. Strukul, *J. Phys. Chem. B* **1998**, *102*, 5733.

[10] I. Yagi, T. Ishida, K. Uosaki, *Electrochem. Commun.* **2004**, *6*, 773.

[11] J. Hernandez, J. Solla-Gullon, E. Herrero, A. Aldaz, J. M. Feliu, *J. Phys. Chem. C* **2007**, *111*, 14078.

[12] M. Haruta, *Catal. Today* **1997**, *36*, 153.

[13] W. Tang, H. F. Lin, A. Kleiman-Shwarsctein, G. D. Stucky, E. W. McFarland, *J. Phys. Chem. C* **2008**, *112*, 10515.

[14] A. A. Herzing, C. J. Kiely, A. F. Carley, P. Landon, G. J. Hutchings, *Science* **2008**, *321*, 1331.

[15] R. L. Whetten, J. T. Khoury, M. M. Alvarez, S. Murthy, I. Vezmar, Z. L. Wang, P. W. Stephens, C. L. Cleveland, W. D. Luedtke, U. Landman, *Adv. Mater.* **1996**, *8*, 428.

[16] T. G. Schaaff, M. N. Shafigullin, J. T. Khoury, I. Vezmar, R. L. Whetten, W. G. Cullen, P. N. First, C. GutierrezWing, J. Ascensio, M. J. JoseYacaman, *J. Phys. Chem. B* **1997**, *101*, 7885.

[17] V. L. Jimenez, D. G. Georganopoulou, R. J. White, A. S. Harper, A. J. Mills, D. I. Lee, R. W. Murray, *Langmuir* **2004**, *20*, 6864.

[18] Y. Shichibu, Y. Negishi, T. Tsukuda, T. Teranishi, *J. Am. Chem. Soc.* **2005**, *127*, 13464.

[19] H. Tsunoyama, Y. Negishi, T. Tsukuda, *J. Am. Chem. Soc.* **2006**, *128*, 6036.

[20] J. B. Tracy, G. Kalyuzhny, M. C. Crowe, R. Balasubramanian, J. P. Choi, R. W. Murray, *J. Am. Chem. Soc.* **2007**, *129*, 6706.

[21] A. Dass, A. Stevenson, G. R. Dubay, J. B. Tracy, R. W. Murray, *J. Am. Chem. Soc.* **2008**, *130*, 5940.

[22] A. Dass, G. R. Dubay, C. A. Fields-Zinna, R. W. Murray, *Anal. Chem.* **2008**, *80*, 6845.

[23] R. C. Jin, S. Egusa, N. F. Scherer, *J. Am. Chem. Soc.* **2004**, *126*, 9900.

[24] S. Trasatti, O. A. Petrii, *Pure Appl. Chem.* **1991**, *63*, 711.

[25] J. J. Pireaux, M. Liehr, P. A. Thiry, J. P. Delrue, R. Caudano, *Surf. Sci.* **1984**, *141*, 221.

[26] J. A. van Bokhoven, J. T. Miller, *J. Phys. Chem. C* **2007**, *111*, 9245.

[27] N. S. Phala, E. van Steen, *Gold Bull.* **2007**, *40*, 150.

[28] L. Barrio, P. Liu, J. A. Rodriguez, J. M. Campos-Martin, J. L. G. Fierro, *J. Phys. Chem. C* **2007**, *111*, 19001.

[29] A. Sarapuu, M. Nurmik, H. Mandar, A. Rosental, T. Laaksonen, K. Kontturi, D. J. Schiffrin, K. Tammeveski, *J. Electroanal. Chem.* **2008**, *612*, 78.

[30] R. E. Davis, G. L. Horvath, C. W. Tobias, *Electrochim. Acta* **1967**, *12*, 287.

[31] M. S. El-Deab, K. Arihara, T. Ohsaka, *J. Electrochem. Soc.* **2004**, *151*, E213.

[32] K. P. Gong, F. Du, Z. H. Xia, M. Durstock, L. M. Dai, *Science* **2009**, *323*, 760.